Optomechanical thermal intermodulation noise

S. A. Fedorov,[1,*] A. Beccari,[1,*] A. Arabmoheghi,[1] D. J. Wilson,[2] N. J. Engelsen,[1] and T. J. Kippenberg[1,†]

[1] *Institute of Physics (IPHYS), École Polytechnique Fédérale de Lausanne, 1015 Lausanne, Switzerland*
[2] *College of Optical Sciences, University of Arizona, Tucson, Arizona 85721, USA*

(Dated: February 27, 2020)

Thermal fluctuations give rise to noise processes in optical interferometers, limiting the sensitivity of precision measurements ranging from the detection of gravitational waves to the stabilization of lasers for optical atomic clocks. In optical cavities, thermal fluctuations of length and refractive index result in cavity frequency noise, which couples to the optical field. Here we describe a noise process, thermal intermodulation noise, produced by the inherent nonlinearity of optical susceptibility in laser-cavity detuning. We study thermal intermodulation noise due to the Brownian motion of membrane resonators in membrane-in-the-middle optomechanical cavities at room temperature, and show it to be the dominant source of classical intracavity intensity fluctuations under nearly-resonant optical excitation. We are able to operate at nominal quantum cooperativity equal to one an optomechanical cavity with optical finesse $\mathcal{F} = 1.5 \times 10^4$ and a low effective mass soft clamped membrane mode with $Q = 4.1 \times 10^7$ as a mechanical oscillator. In this regime, the thermal intermodulation noise created by the mixing products of membrane modes exceeds the vacuum fluctuations by orders of magnitude, preventing the observation of pondermotive squeezing. The described noise process is broadly relevant to optical cavities, especially to those in which thermal frequency fluctuations are not negligible compared to the optical linewidth.

I. INTRODUCTION

Optical cavities are ubiquitous in physical experiments. They are used for precision interferometric position measurements, an extraordinary example of which is direct gravitational wave detection[1], ultrastable lasers[2], and quantum experiments, including cavity quantum electrodynamics[3] and optiomechanics[4]. Optical cavities have finite temperature and therefore their frequencies exhibit fundamental thermal fluctuations due to the Brownian motion of mirror surfaces, thermorefractive and thermoelastic fluctuations[5, 6] and other processes that modulate the effective cavity length. These fluctuations predominantly manifest as excess phase noise in an optical field resonant with the cavity. At the same time, the nonlinearity of cavity discrimination curve creates intensity noise in the resonant field, which is especially pronounced when the magnitude of frequency fluctuations is comparable to the optical linewidth. This effect is known as intermodulation noise as it mixes different harmonics of the frequency noise. Technical intermodulation noise is known to limit the stability of frequency standards[7] and cavity-stabilized lasers[8, 9]. Here we report and study thermal intermodulation noise (TIN) that has fundamental thermodynamic origin.

The transduction of optical path difference into measured signal in optical interferometers is periodic with the period equal to wavelength, λ, and therefore inherently nonlinear. Correspondingly, an optical cavity transduces the fluctuations of round-trip optical path, δl, to the modulation of intracavity field linearly only as far as the fluctuations of phase shift,

$$\delta\phi = \mathcal{F}\delta l/\lambda, \tag{1}$$

accumulated over the light storage time, are much smaller than one. Therefore high optical finesse not only increases the resolution of a cavity as an optical path sensor but also limits its dynamic range to $\lambda/\mathcal{F}$[10, 11]. This is an important consideration in experiments in which, on one hand, high finesse is desirable to increase the strength of light-matter interaction, and, on the other hand, stringent constraints exist on the tolerable level of extraneous noise in both quadratures of the optical field. Experiments on quantum cavity optomechanics are among such.

Quantum cavity optomechanics studies aspects of interaction between optical field and mechanical motion such as position measurements and feedback control in presence of measurement backaction[12, 13], the preparation of mechanical ground[14–16], single-phonon[17] and entangled[18] states, and ponderomotive squeezing[19, 20]. In a handful of recent experiments, some quantum optomechanical effects were demonstrated at room temperature[21–25], limited due to high thermal noise levels. Most of these experiments[23–25] operated in an exotic regime when the radiation pressure spring exceeded the natural frequency of the mechanical oscillator by two orders of magnitude.

An alternative platform which is considered promising for quantum optomechanics at room temperature is membrane-in-the-middle (MiM) system[26, 27]. It is predicted that quantum-backaction dominated regime is reacheable at microwatt input optical powers with the help of recently developed high-stress Si_3N_4 membrane resonators hosting high-Q and low mass soft-clamped modes[28, 29]. Yet, concomitant with this approach is a dense spectrum of membrane modes, which equally couple to the optical field and produce large frequency

* These authors contributed equally
† tobias.kippenberg@epfl.ch

fluctuations, proportional to the temperature, T. The nonlinear thermal intermodulation noise, associated with these fluctuations, is $\propto T^2$, and therefore particularly strong at room temperature.

The optical transduction nonlinearity that creates thermal intermodulation noise was reported in optomechanical systems previously[30, 31]. To the lowest order in the displacement over dynamic range, it manifests as the measurement of mechanical displacement squared. Such measurements potentially have enticing applications in quantum optomechanics, they can be used for the observation of phononic jumps[32], phononic shot noise[33], and the creation of mechanical squeezed states[34] if the effects of linear measurement backaction are possible to keep small[30, 35]. Experiments that demonstrated demonstrating quadratic optomechanical position measurements using position-squared coupling to the cavity frequency[36] up to date remain deeply in the classical regime because of the small coupling rates. Optical cavity transduction can produce effective quadratic nonlinearity that is orders of magnitude higher[30], but it is inevitably accompanied by linear quantum backaction.

The manuscript is structured as follows. In the beginning we introduce a theoretical model of thermal intermodulation noise. Next we present measurements in low-cooperativity regime which reveal an extraneous intensity noise source in a resonantly driven membrane-in-the-middle cavity. We show the noise to match the expected from the model magnitude and scaling with optical linewidth. Finally, employing a PnC membrane with a low effective mass soft clamped mode we conduct measurements in the onset of quantum backaction-dominated regime. We study the dependence of TIN on laser detuning, and find it to be in excellent agreement with our theoretical prediction. Moreover, we show that TIN is a significant limitation for the observability of quantum backaction-imprecision correlations.

II. THEORY OF INTERMODULATION NOISE

We begin by presenting the theory of thermal intermodulation noise in an optical cavity under the assumption that the frequency fluctuations are slow compared to the optical decay rate. We concentrate on the lowest-order, i.e. quadratic, nonlinearity of the cavity detuning transduction.

Consider an optical cavity with two-ports which is driven by a laser coupled to port one and the output from port two of which is directly detected on a photodiode. In the classical regime, i.e. neglecting vacuum fluctuations, the intracavity optical field, a, and the output field $s_{\mathrm{out},2}$ are found from the equations

$$\frac{da(t)}{dt} = \left(i\Delta(t) - \frac{\kappa}{2}\right) a(t) + \sqrt{\kappa_1}\, s_{\mathrm{in},1}, \tag{2}$$

$$s_{\mathrm{out},2}(t) = -\sqrt{\kappa_2} a(t). \tag{3}$$

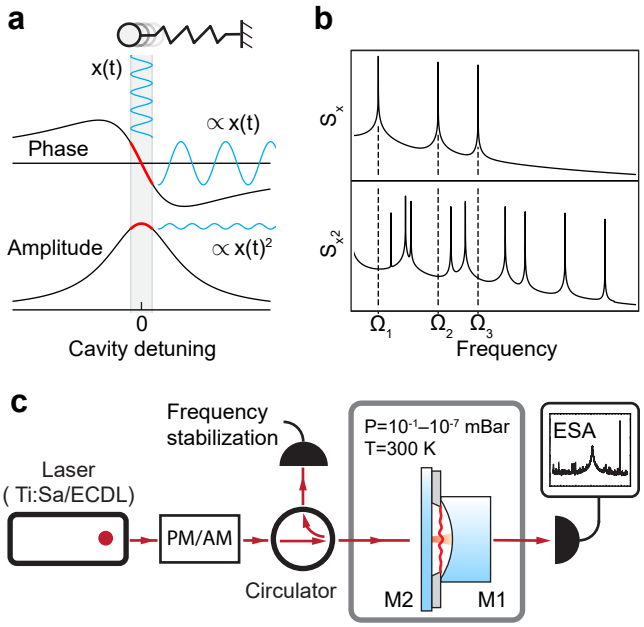

FIG. 1. a) Transduction of the oscillator motion to the phase (upper panel) and amplitude (lower panel) quadratures of resonant intracavity light. b) Spectra of linear (upper panel) and quadratic (lower panel) position fluctuations of a multimode resonator. c) Experimental setup.

where $s_{\mathrm{in},1}$ is the constant coherent drive amplitude, $\Delta(t) = \omega_L - \omega_c(t)$ is the laser detuning from the cavity resonance, modulated by the cavity frequency noise, and $\kappa_{1,2}$ are the coupling rates of the ports one and two. Observe that it follows from Eq. 3 that the intensity of the detected light is directly proportional to the intracavity intensity. In the fast cavity limit, when the optical field adiabatically follows $\Delta(t)$, the intracavity field is found as

$$a(t) = 2\sqrt{\frac{\eta_1}{\kappa}} L(\nu(t))\, s_{\mathrm{in},1}, \tag{4}$$

where we introduced for brevity the normalized detuning $\nu = 2\Delta/\kappa$, the cavity decay ratios $\eta_{1,2} = \kappa_{1,2}/\kappa$ and Lorentzian susceptibility

$$L(\nu) = \frac{1}{1 - i\nu}. \tag{5}$$

Expanding L in Eq. 4 over small detuning fluctuations $\delta\nu$ around the mean value ν_0 up to the second order we find the intracavity field as

$$a = 2\sqrt{\frac{\eta_1}{\kappa}} L(\nu_0)(1 + iL(\nu_0)\delta\nu - L(\nu_0)^2\delta\nu^2) s_{\mathrm{in},1}. \tag{6}$$

According to Eq. 6, the intracavity field is modulated by the cavity frequency excursion, $\delta\nu$, and the frequency excursions squared, $\delta\nu^2$. If $\delta\nu(t)$ is a stationary Gaussian noise process, like a thermal noise, the linear and quadratic contributions are uncorrelated (despite clearly not

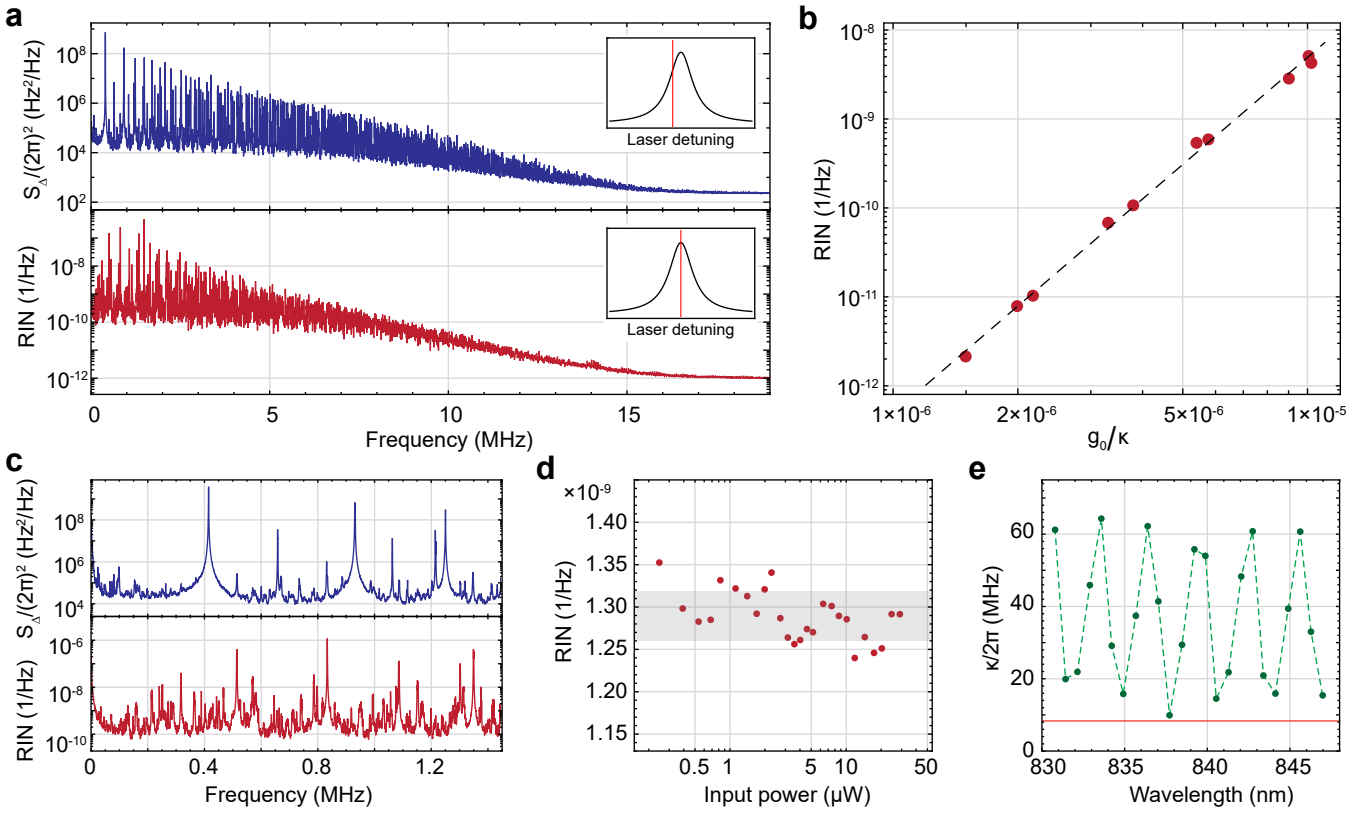

FIG. 2. a) Noise from a MiM cavity with laser detuned from resonance and on resonance. 1 mm square membrane, $\kappa/2\pi = 26.6$ MHz, $g_0/2\pi = 330$ Hz. c) The low frequency part of data in a). b), d) and e) show measurements for MiM cavity with 2 mm square membrane. b) dependence of the average RIN in $0.6-1.6$ MHz band. b) Power sweep on the resonance with wavelength 837.7 nm, band ± one standard deviation around the mean is shaded gray. e) Green points — measured linewidths of different optical resonances of MiM cavity, the dashed line is a guide to eye. Orange line — linewidth of an empty cavity with the same length.

being independent). This is due to the fact that odd-order correlations vanish for Gaussian noise,

$$\langle \delta\nu(t)^2 \delta\nu(t+\tau)\rangle = 0, \tag{7}$$

where $\langle ...\rangle$ is time-average, for arbitrary time delay τ.

Next, we consider the ptotodetected signal, which, up to an unimportant conversion factor, equals to the intensity of the output light and found as

$$I(t) = |s_{\text{out},2}(t)|^2 \propto |L(\nu_0)|^2 \left(1 - \frac{2\nu_0}{1+\nu_0^2}\delta\nu(t) + \frac{3\nu_0^2-1}{(1+\nu_0^2)^2}\delta\nu(t)^2\right). \tag{8}$$

Notice, that $\nu(t)$ and $\nu(t)^2$ can be independently measured at different detunings ν_0. Whereas the linearly transduced term vanishes on resonance ($\nu = 0$), there are also "magic" detunings, $\nu_0 = \pm 1/\sqrt{3}$, at which quadratic frequency fluctuations do not contribute to the detected signal and therefore the intermodulation noise vanishes to the leading order.

The spectrum of the detected signal is an incoherent sum of linear term,

$$S_{\nu\nu}[\omega] = \int_{-\infty}^{\infty} \langle \delta\nu(t)\delta\nu(t+\tau)\rangle e^{i\omega\tau} d\tau, \tag{9}$$

and quadratic term, which for Gaussian noise can be found using the Wick's theorem[37]

$$\langle \delta\nu(t)^2 \delta\nu(t+\tau)^2\rangle = \langle \delta\nu(t)^2\rangle^2 + 2\langle \delta\nu(t)\delta\nu(t+\tau)\rangle^2, \tag{10}$$

as

$$S_{\nu\nu,2}[\omega] = \int_{-\infty}^{\infty} \langle \delta\nu(t)^2\delta\nu(t+\tau)^2\rangle e^{i\omega\tau} d\tau = 2\pi\langle\delta\nu^2\rangle^2\delta[\omega] + 2\times\frac{1}{2\pi}\int_{-\infty}^{\infty} S_{\nu\nu}[\omega']S_{\nu\nu}[\omega-\omega']d\omega', \tag{11}$$

where δ is delta-function.

III. THERMOMECHANICAL INTERMODULATION NOISE

In an optomechanical cavity the dominant source of cavity frequency fluctuations is the Brownian motion of

mechanical modes coupled to the cavity,

$$\delta\nu(t) = 2\frac{G}{\kappa}x(t), \tag{12}$$

where $G = -\partial\omega_c/\partial x$ is the linear optomechanical coupling constant, and x is the total resonator displacement, the sum of independent contributions x_n of different mechanical modes. The spectrum of Brownian frequency noise is found as

$$S_{\nu\nu}[\omega] = \left(\frac{2G}{\kappa}\right)^2 \sum_n S_{xx,n}[\omega], \tag{13}$$

where $S_{xx,n}[\omega]$ are the displacement spectra of individual mechanical modes (see SI for more details). Applied to $S_{\nu\nu}$ given by Eq. 13, the convolution in Eq. 11 describes thermomechanical intermodulation noise with peaks at sums and differences of mechanical resonance frequencies, together with broadband background due to off-resonant components of thermal noise, as illustrated in Fig. 1b. The magnitude of intermodulation noise is related to the quadratic spectrum of total mechanical displacement, $S_{xx,2}$, as

$$S_{\nu\nu,2} = (2G/\kappa)^4 S_{xx,2}. \tag{14}$$

A reservation needs to be made, that the theory presented in Sec. II, is only strictly applicable to an optomechanical cavity at low enough optical power at which the driving of mechanical motion by radiation pressure fluctuations created by the intermodulaton noise is negligible; otherwise the fluctuations of $x(t)$ and $\delta\nu(t)$ may deviate from purely Gaussian and correlations exist between $S_{\nu\nu}$ and $S_{\nu\nu,2}$. On the practical level, this reservation has minor significance for our experiment. Also, the presence of linear dynamical backaction of radiation pressure does not change the results of Sec. II but only modifies S_{xx}.

Thermal intermodulation noise obscures linear quantum correlations, which are induced by the vacuum fluctuations of radiation pressure between the quadratures of intracavity field and manifest as ponderomotive squeezing[19, 20], Raman sideband asymmetry[12] and the cancellation of shot noise in force measurements[22, 38]. The observation of these effects typically requires picking one mechanical mode with high vacuum coupling rate, g_0, and spectral neighbourhood clean from extraneous thermal noises. The vacuum coupling rate for the mode is defined as

$$g_0 = Gx_{\mathrm{zpf}}, \tag{15}$$

where $x_{\mathrm{zpf}} = \sqrt{\hbar/2m_{\mathrm{eff}}\Omega_m}$ is the magnitude of zero point fluctuations, Ω_m is the mechanical resonance frequency and m_{eff} is the effective mass. The onset of quantum regime of linear optomechanical interaction happens when the quantum cooperativity, C_q, reaches unity,

$$C_q = \frac{4g_0^2}{\kappa\Gamma_{\mathrm{th}}}n_c \sim 1. \tag{16}$$

Here n_c is the mean intracavity photon number, κ is the optical linewidth and $\Gamma_{\mathrm{th}} = \Gamma_m n_{\mathrm{th}}$ is the mechanical thermal decoherence rate equal to the product of mechanical energy relaxation rate and the oscillator phonon occupancy. The condition for the intermodulation noise in the amplitude quadrature to be negligible compared to the vacuum fluctuations is given by

$$C_q\left(\frac{g_0}{\kappa}\right)^2\Gamma_{\mathrm{th}}\frac{S_{xx,2}[\omega]}{x_{\mathrm{zpf}}^4} \ll 1. \tag{17}$$

The nonlinearity of optical detuning transduction modulates the optical field proportional to x^2 in way analogous, but not equivalent, to the nonlinear optomechanical coupling, $\partial^2\omega_c/\partial x^2$. It was noticed[30] that the cavity transduction commonly has nonlinearity that is orders of magnitude stronger than the highest experimentally reported $\partial^2\omega_c/\partial x^2$, when compared by the magnitude of the optical signal proportional to x^2. In the Supplementary Information it is shown that the same is true for membrane-in-the-middle cavity, in which typical quadratic signals originating from the nonlinear transduction and leading to intermodulation noise are by the factor of $r\mathcal{F}$ (where r is membrane reflectivity) larger than the signals due to the nonlinear optomechanical coupling, $\partial^2\omega_c/\partial x^2$.

IV. EXPERIMENTAL OBSERVATION OF EXTRANEOUS AMPLITUDE NOISE

TIN has a number of manifestations that are qualitatively different from other thermal noises in optical cavities. In particular, TIN is present in the amplitude quadrature of optical field coupled to a cavity on resonance, and its magnitude depends very sensitively on the ratio of RMS cavity frequency fluctuations over the linewidth. In this section we present the observation of broadband classical intensity noise in the optical field resonant with membrane-in-the-middle optomechanical cavity at room temperature, and verify that this noise is due to the intermodulation of Brownian motion of membrane modes.

Our experimental setup, shown in Fig. 1c, incorporates a membrane-in-the-middle cavity, consisting of two dielectric high-reflectivity mirrors with 100 ppm transmission and a 200 μm-thick silicon chip which is sandwiched directly between the mirrors and hosts a suspended high-stress stoichiometric Si_3N_4 membrane. The total length of the cavity is around 350 μm. The MiM cavity is situated in a vacuum chamber at room temperature and probed using a Ti:Sa or a tunable ECDL laser at wavelength around 840 nm, close to the maximum reflectivity wavelength of the mirrors. The Ti:Sa laser was used in all the thermal noise measurements, whereas the diode laser was only used for the characterization of optical linewidths. The direct detection of light transmitted through the cavity on an avalanche photodiode generated the measurement signal, the reflected light, separated using a

circulator, was used for PDH locking of the Ti:Sa frequency. The spectra of signals, detected in transmission, were calibrated either as relative intensity noise (RIN) or as effective cavity detuning fluctuations with the help of calibration tones applied to the amplitude or phase quadratures of the laser, respectively.

The characterization of TIN was performed using 20 nm-thick square membranes of different sizes as mechanical resonators. The insertion of a membrane in the cavity resulted in excess loss for most of the optical resonances, nevertheless some resonances retained their optical quality factors with as little as 10%[check this number] added loss. A typical variation of optical loss rate with wavelength is shown in Fig. 2e for a cavity with 2mm×2mm membrane. The optomechanical cooperativity was kept low during the noise measurements in order to eliminate the dynamical backaction of light (cooling or amplification of mechanical motion). For this purpose the residual pressure in the vacuum chamber was kept high, 0.22 ± 0.03 mBar, so that the quality factors of the fundamental modes of membranes were limited by the gas damping to $Q \sim 10^3$.

Fig. 2a and c show typical spectra of the photodetected signals taken with 1mm×1mm square membrane. When the laser is locked detuned from the cavity resonance (close to the "magic" detuning, $\nu_0 \approx -1/\sqrt{3}$), the transmission signal is dominated by the Brownian motion of membrane modes linearly transduced by the cavity. The magnitude of thermomechanical noise is gradually reduced at high frequencies due to the averaging of membrane mode profiles[40, 41] over the cavity waist (approx 25 μm in our experiment), until it meets shot noise at around 15 MHz, which is proved by examining the optical power dependence (see SI). When the laser is locked on resonance, the output light also contains a wast amount of thermal noise—at the input power of 5 μW the classical RIN exceeds the shot noise level by about 25 dB at MHz frequencies. Again, at high frequency the noise level approaches shot noise.

An unambiguous proof of the intermodulation origin of the resonant intensity noise is obtained from examining the scaling of noise level with G/κ. In thermal equilibrium the spectral density of relative frequency fluctuations created by a particular membrane is $\propto (G/\kappa)^2$, and therefore the spectral density of intermodulation noise is expected to be $\propto (G/\kappa)^4$. We confirm this scaling by measuring the resonant intensity noise for different optical modes of a cavity with a 2mm×2mm membrane and plotting in Fig. 2b the noise, averaged over the frequency band 0.6-1.6 MHz, as a function of g_0/κ. Here g_0 is that of the fundamental mechanical mode, measured using the method of Ref. [42]. By performing a sweep of the input laser power on one of the resonances of the same cavity we show (see Fig. 2d) that the resonant intensity noise level is power-independent and therefore the noise is not related to radiation pressure effects.

The TIN observed in our experiment is well reproduced theoretically, by calculating the spectrum of total

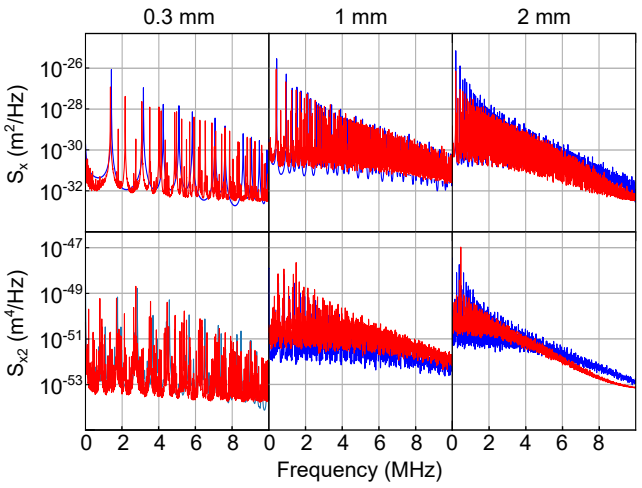

FIG. 3. Effective (averaged over the cavity mode profile) displacement (top row) and displacement squared (bottom row) noises produced by the modes of 20-nm Si_3N_4 rectangular membranes of different sizes. Red is experimental data and blue is theoretical prediction. (Warning: two-sided theory spectra might be plotted, also the data for 2 mm membrane should be replaced) [also need to remove the cavity delay correction]

membrane fluctuations according to Eq. 13 and applying the convolution formula from Eq. 11 (see SI for full details). In Fig. 3, we compare with theory the linear and quadratic displacement spectra of membranes of different sizes. Instead of comparing directly $S_{\nu\nu}$ and resonant RIN noises detected in the experiment, we convert them to S_{xx} and $S_{xx,2}$, respectively, using independently measured κ and g_0 of the fundamental mechanical mode and assuming the theoretical value for its $m_{\rm eff}$. Such calibration provides a better insight in the variation of noise levels with membrane size as optical noises are also dependent on G/κ, which was different in different measurements. In the theoretical model for simplicity we assume the quality factors of all membrane modes are the same. While such model is not detailed enough to reproduce precisely all noise features, it well reproduces the overall magnitude and the broadband envelope of the intermodulation noise observed in experiment. It is evident from Fig. 3 that larger membranes produce larger total quadratic fluctuations, and therefore stronger TIN at the same G/κ.

[Mention that the laser locking does not affect the intermodulation noise]

[Add discussion that the potential dissipative coupling can only produce a much weaker effect on the intermodulation noise]

[Give estimates of rms frequency fluctuations, maybe also a plot with transmission over a resonance?]

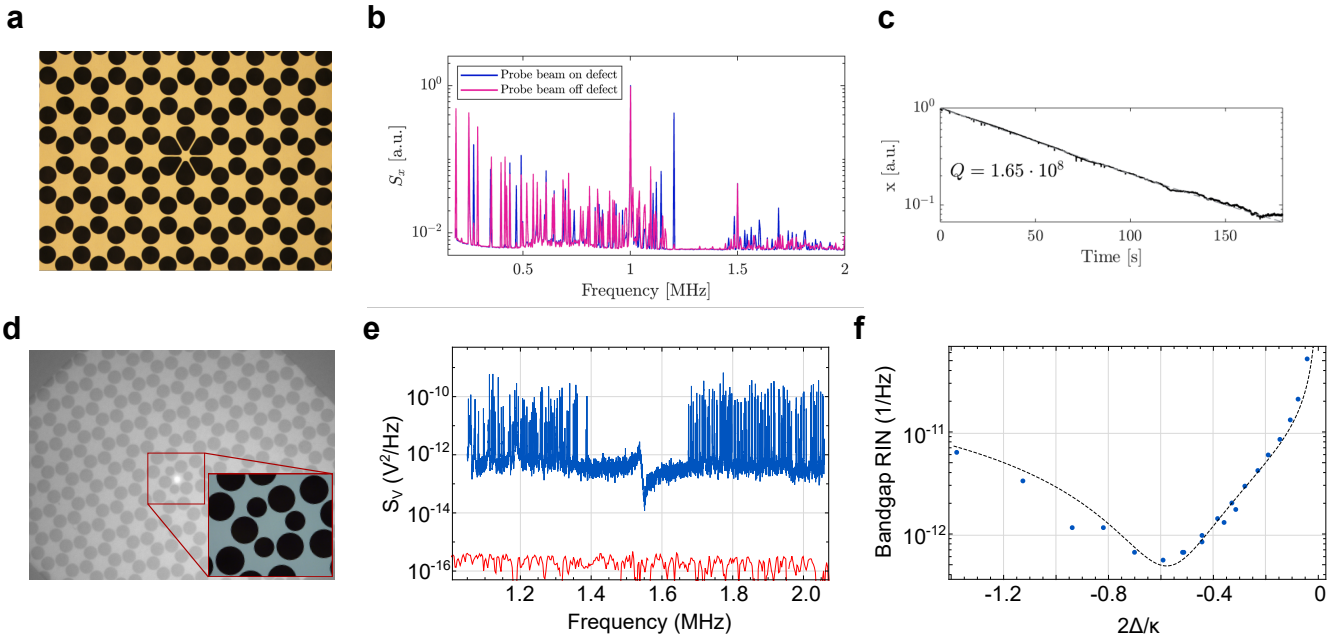

FIG. 4. a) Microscope image of a 3.6mm ×3.3mm × 20nm, with a low m_{eff} localized mode frequency of approximately 800 kHz, b) displacement spectrum of the membrane in a(replace data for this to be true) c) ringdown measurement of quality factor of the membrane in a. d) Microscope image of a 2mm × 2mm × 20nm membrane hosting a soft clamped mode. e) Blue—protocurrent noise spectrum detected with laser detuned from the cavity resonance, red—shot noise level. f) The variation of the relative intensity noise of the light output from MiM cavity at bandgap frequencies with laser-cavity detuning. Blue dots are experimental points, dashed line - single-parameter model fit.

V. MIM CAVITY WITH PHONONIC CRYSTAL MEMBRANE

As was discovered recently[28], MHz frequency localized ("soft clamped") defect modes in stressed phononic crystal (PnC) resonators can have quality factors in excess of 10^8 at room temperature due to the enhancement of dissipation dilution[28, 43]. In PnC membranes, soft-clamped modes with thermal force noises[44], $S_{\text{FF,th}}$, down to 55 aN/$\sqrt{\text{Hz}}$ at room temperature were demonstrated previously[28, 29].

In Fig ... a and b we present 20 nm-thick Si_3N_4 PnC membranes with soft-clamped modes optimized for low effective mass and high Q. The phononic crystal is formed by a hexagon pattern of circular holes, introduced in Ref. [28], which creates complete phononic bandgap for flexural modes. The phononic crystal is terminated to the silicon frame at half the hole radii in order to prevent mode localization at the membrane edges—such modes are low-Q and can have frequencies withing the phononic bandgap, contaminating the spectrum. Fig ... a shows the microscope image of a resonator with trampoline defect, featuring $m_{\text{eff}} = 1.9$ ng at $\Omega_m/2\pi = 0.853$ kHz and $Q = 1.65 \times 10^8$, corresponding to the force noise of $S_{\text{FF,th}} = 15$ aN/$\sqrt{\text{Hz}}$. Another design, shown in Fig ... b , is a 2mm×2mm phononic crystal membrane with defect that was engineered to create a single mode localized in the middle of phononic bandgap. The shown sample featured $Q = 7.4 \times 10^7$ at 1.46 MHz and $m_{\text{eff}} = 1.1$ ng, corresponding to $S_{\text{FF,th}} = 34$ aN/$\sqrt{\text{Hz}}$. The membrane designs found in[45].

Phononic bandgap spectrally isolates soft-clamped modes from the thermomechanical noise created by the rest of the membrane spectrum. Nevertheless, when a PnC membrane is incorporated in a MiM cavity the entire multitude of membrane modes contributes to the TIN at bandgap frequencies, as TIN is produced by a nonlinear process. In the following we present measurements of in-bandgap excess nose in a MiM cavity at room temperature and show that it is dominated by TIN at all detunings except for the immediate vicinity of the "magic" detuning $\nu_0 = -1/\sqrt{3}$. Around $\nu_0 = -1/\sqrt{3}$ the thermal noise of the cavity mirrors is the dominant excess noise. The measurements were conducted using a PnC membrane with the design shown in Fig ... b, but made of 40 nm-thick Si_3N_4 , which has a single soft-clamped mode with $Q = 4.1 \times 10^7$ at 1.55 MHz. The setup was the same as described in Sec. IV and shown in Fig. 1c, the only difference is that the vacuum pressure was below 5×10^{-7} mBar to eliminate the gas damping of mechanical motion.

[*****The text is unedited below in anticipation of updated figures*****]

Using the membrane shown in Fig. 4d we were able to reproducibly assemble membrane-in-the-middle cavities with single-photon cooperativity $C_0 = 0.1 - 1$ and round trip added loss lower than 200 ppm. For such cavities the

quantum backaction-dominated regime is expected to be reached at the input powers of a few hundreds of μW.

Fig. 4e shows the spectrum of light output from a membrane-in-the-middle cavity with length around 350 μm, $g_0/2\pi = 360$ Hz, $\kappa/2\pi = 24.8$ MHz (giving an estimate of the added optical round trip loss around 100 ppm). The laser was detuned to the red from the cavity resonance in this measurement, and the spectrum of output fluctuations contains both the contribution of thermomechanical noise linearly transduced by the cavity detuning and the intermodulation noise due to the nonlinearity in G/κ. In particular, at frequencies within the phononic bandgap the noise level is dominated by the intermodulation noise, which rises almost 40 dB above the level of vacuum fluctuations (calibrated separately by directing an auxiliary laser beam of the the same power on the detector). The intermodulation origin of the noise in the bandgap can be proven by considering the variation of the noise level with laser detuning presented in Fig. 4f. The laser power in this measurement was kept fixed to 30 μW, the cavity resonance wavelength is 840.1 nm.

We can understand the data in Fig. 4f using the general formula for the photocurrent produced in the detection of outgoing light (Eq. 8). Linear and quadratic position fluctuations are transduced differently by the cavity, but almost within the entire range of the detunings the quadratically transduced fluctuations dominate. The exception is the vicinity of the detuning $\Delta = \kappa/(2\sqrt{3})$ at which the quadratic transduction by the cavity is compensated by the quadratic transduction by the nonlinearity of photodetection (see SI for discussion). At this detuning the in-bandgap noise level is consistent with the mirror noise. The overall variation of noise with the detuning can be described by the formula

$$S_{\rm II} \propto \frac{4\nu_0^2}{(1+\nu_0^2)^2} S_{\nu\nu} + \frac{1}{\nu_0}\frac{(3\nu_0^2-1)^2}{1+\nu_0^2} S_{\nu\nu,2}, \qquad (18)$$

where S_1 is the contribution of mirror noise, which is independently calibrated, and S_2 is the contribution of quadratic noise that we use as a fitting parameter for the dashed curve in Fig. 4f. Aside from the cavity transduction, Eq. 18 takes into account the laser cooling of mechanical modes by dynamic backaction (assuming that the optical damping is much larger than the intrinsic linewidth, see SI for details). As can be seen from Fig. 4f, Eq. 18 very well reproduces the experimental data.

[Mention that at the magic detuning the contribution of TIN to the intracavity radiation pressure noise is also zero]

[Mention that the effect of mirror noise could be suppressed by operation close to the resonance]

VI. CONCLUSIONS AND OUTLOOK

The suppression of intermodulation noise can be done by engineering mechanical resonators with lower multimode thermal noise and fewer modes, or by using optomechanical cavities with lower g_0/κ.

As a potential way to suppress the intermodulation noise we may suggest engineering the optical susceptibility in a way that the quadratic transduction vanishes, for example, using double resonance.

VII. ACKNOWLEDGEMENTS

The authors thank Ryan Schilling for fabrication advice. All samples were fabricated and grown in the Center of MicroNanoTechnology (CMi) at EPFL. This work was supported by the Swiss National Science Foundation under grant no. 182103 and the Defense Advanced Research Projects Agency (DARPA), Defense Sciences Office (DSO), under contract no. D19AP00016 (QUORT). A.B. acknowledges support from the European Union's Horizon 2020 research and innovation program under the Marie Sklodowska-Curie grant agreement no. 722923 (OMT). N.J.E. acknowledges support from the Swiss National Science Foundation under grant no. 185870 (Ambizione).

[1] LIGO Scientific Collaboration and Virgo Collaboration, Physical Review Letters **116**, 061102 (2016).
[2] U. Sterr, T. Legero, T. Kessler, H. Schnatz, G. Grosche, O. Terra, and F. Riehle, in *Time and Frequency Metrology II*, Vol. 7431 (International Society for Optics and Photonics, 2009) p. 74310A.
[3] J. Ye, H. J. Kimble, and H. Katori, Science **320**, 1734 (2008), publisher: American Association for the Advancement of Science Section: Review.
[4] M. Aspelmeyer, T. J. Kippenberg, and F. Marquardt, Reviews of Modern Physics **86**, 1391 (2014).
[5] V. B. Braginsky, M. L. Gorodetsky, and S. P. Vyatchanin, Physics Letters A **271**, 303 (2000).
[6] M. L. Gorodetsky, Physics Letters A **372**, 6813 (2008).
[7] C. Audoin, V. Candelier, and N. Diamarcq, IEEE Transactions on Instrumentation and Measurement **40**, 121 (1991).
[8] B. A. Ferguson and D. S. Elliott, Physical Review A **41**, 6183 (1990).
[9] M. Bahoura and A. Clairon, IEEE Transactions on Ultrasonics, Ferroelectrics, and Frequency Control **50**, 1414 (2003).
[10] H. Miao, S. Danilishin, T. Corbitt, and Y. Chen, Physical Review Letters **103**, 100402 (2009).
[11] F. Khalili, S. Danilishin, H. Miao, H. Mller-Ebhardt, H. Yang, and Y. Chen, Physical Review Letters **105**, 070403 (2010).
[12] V. Sudhir, D. Wilson, R. Schilling, H. Schtz, S. Fedorov, A. Ghadimi, A. Nunnenkamp, and T. Kippenberg, Phy-

sical Review X **7**, 011001 (2017).
[13] D. J. Wilson, V. Sudhir, N. Piro, R. Schilling, A. Ghadimi, and T. J. Kippenberg, Nature **524**, 325 (2015).
[14] J. Chan, T. P. M. Alegre, A. H. Safavi-Naeini, J. T. Hill, A. Krause, S. Grblacher, M. Aspelmeyer, and O. Painter, Nature **478**, 89 (2011).
[15] L. Qiu, I. Shomroni, P. Seidler, and T. J. Kippenberg, arXiv:1903.10242 [quant-ph] (2019), arXiv: 1903.10242.
[16] M. Rossi, D. Mason, J. Chen, Y. Tsaturyan, and A. Schliesser, Nature **563**, 53 (2018).
[17] S. Hong, R. Riedinger, I. Marinkovi, A. Wallucks, S. G. Hofer, R. A. Norte, M. Aspelmeyer, and S. Grblacher, Science (2017), 10.1126/science.aan7939.
[18] R. Riedinger, A. Wallucks, I. Marinkovi, C. Lschnauer, M. Aspelmeyer, S. Hong, and S. Grblacher, Nature **556**, 473 (2018).
[19] A. H. Safavi-Naeini, S. Grblacher, J. T. Hill, J. Chan, M. Aspelmeyer, and O. Painter, Nature **500**, 185 (2013).
[20] T. P. Purdy, P.-L. Yu, R. W. Peterson, N. S. Kampel, and C. A. Regal, Physical Review X **3** (2013), 10.1103/PhysRevX.3.031012.
[21] T. P. Purdy, K. E. Grutter, K. Srinivasan, and J. M. Taylor, arXiv:1605.05664 [cond-mat, physics:physics, physics:quant-ph] (2016), arXiv: 1605.05664.
[22] V. Sudhir, R. Schilling, S. Fedorov, H. Schtz, D. Wilson, and T. Kippenberg, Physical Review X **7**, 031055 (2017).
[23] J. Cripe, N. Aggarwal, R. Lanza, A. Libson, R. Singh, P. Heu, D. Follman, G. D. Cole, N. Mavalvala, and T. Corbitt, Nature **568**, 364 (2019).
[24] M. J. Yap, J. Cripe, G. L. Mansell, T. G. McRae, R. L. Ward, B. J. J. Slagmolen, P. Heu, D. Follman, G. D. Cole, T. Corbitt, and D. E. McClelland, Nature Photonics , 1 (2019).
[25] N. Aggarwal, T. Cullen, J. Cripe, G. D. Cole, R. Lanza, A. Libson, D. Follman, P. Heu, T. Corbitt, and N. Mavalvala, arXiv:1812.09942 [physics, physics:quant-ph] (2018), arXiv: 1812.09942.
[26] J. D. Thompson, B. M. Zwickl, A. M. Jayich, F. Marquardt, S. M. Girvin, and J. G. E. Harris, Nature **452**, 72 (2008).
[27] D. J. Wilson, C. A. Regal, S. B. Papp, and H. J. Kimble, Physical Review Letters **103**, 207204 (2009).
[28] Y. Tsaturyan, A. Barg, E. S. Polzik, and A. Schliesser, Nature Nanotechnology **12**, 776 (2017).
[29] C. Reetz, R. Fischer, G. Assumpo, D. McNally, P. Burns, J. Sankey, and C. Regal, Physical Review Applied **12**, 044027 (2019).
[30] G. A. Brawley, M. R. Vanner, P. E. Larsen, S. Schmid, A. Boisen, and W. P. Bowen, Nature Communications **7**, 10988 (2016).
[31] R. Leijssen, G. R. L. Gala, L. Freisem, J. T. Muhonen, and E. Verhagen, Nature Communications **8**, 1 (2017).
[32] A. A. Gangat, T. M. Stace, and G. J. Milburn, New Journal of Physics **13**, 043024 (2011).
[33] A. A. Clerk, F. Marquardt, and J. G. E. Harris, Physical Review Letters **104**, 213603 (2010).
[34] A. Nunnenkamp, K. Brkje, J. G. E. Harris, and S. M. Girvin, Physical Review A **82**, 021806 (2010).
[35] I. Martin and W. H. Zurek, Physical Review Letters **98**, 120401 (2007).
[36] T. K. Paraso, M. Kalaee, L. Zang, H. Pfeifer, F. Marquardt, and O. Painter, Physical Review X **5**, 041024 (2015).
[37] C. W. Gardiner, *Handbook of Stochastic Methods*, 2nd ed. (Springer, Berlin) section 2.8.1.
[38] N. Kampel, R. Peterson, R. Fischer, P.-L. Yu, K. Cicak, R. Simmonds, K. Lehnert, and C. Regal, Physical Review X **7**, 021008 (2017).
[39] A. B. Matsko and S. P. Vyatchanin, Physical Review A **97**, 053824 (2018).
[40] Y. Zhao, D. J. Wilson, K.-K. Ni, and H. J. Kimble, Optics Express **20**, 3586 (2012), publisher: Optical Society of America.
[41] D. J. Wilson, *Cavity optomechanics with high-stress silicon nitride films*, phd, California Institute of Technology (2012).
[42] M. L. Gorodetksy, A. Schliesser, G. Anetsberger, S. Deleglise, and T. J. Kippenberg, Optics Express **18**, 23236 (2010).
[43] A. H. Ghadimi, S. A. Fedorov, N. J. Engelsen, M. J. Bereyhi, R. Schilling, D. J. Wilson, and T. J. Kippenberg, Science **360**, 764 (2018).
[44] P. R. Saulson, Physical Review D **42**, 2437 (1990).
[45] Raw measurements data, analysis code to repoduce the manuscript figures, and the GDS designs of PnC membranes are available on zenodo.org, DOI:.../zenodo....